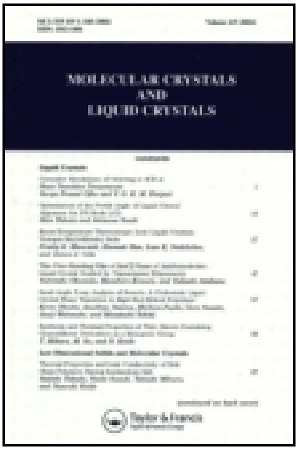

Molecular Crystals and Liquid Crystals

Publication details, including instructions for authors and subscription information:
http://www.tandfonline.com/loi/gmcl16

Raman Scattering by Optical Phonons In $TaSe_3$ and $NbSe_3$

T. J. Wieting [a] , A. Grisel [b] [a] & F. Levy [b] [a]

[a] U.S. Naval Research Laboratory Washington, D.C., 20375

[b] Institut de Physique Appliquee EPFL PHB - Ecublens CH-1015 Lausanne, Switzerland

Version of record first published: 14 Oct 2011.

To cite this article: T. J. Wieting , A. Grisel & F. Levy (1982): Raman Scattering by Optical Phonons In $TaSe_3$ and $NbSe_3$, Molecular Crystals and Liquid Crystals, 81:1, 117-124

To link to this article: http://dx.doi.org/10.1080/00268948208072557

Mol. Cryst. Liq. Cryst., 1982, Vol. 81, pp. 117–124
0026-8941/82/8101-0117$06.50/0

Printed in the United States of America

(Proceedings of the International Conference on Low-Dimensional Conductors, Boulder, Colorado, August 1981)

RAMAN SCATTERING BY OPTICAL PHONONS IN $TaSe_3$ AND $NbSe_3$

T.J. Wieting
U.S. Naval Research Laboratory
Washington, D.C. 20375

A. Grisel and F. Levy
Institut de Physique Appliquee EPFL
PHB - Ecublens
CH-1015 Lausanne, Switzerland

Received for publication August 31, 1981

Room-temperature Raman spectra have been obtained between 20 cm^{-1} and 400 cm^{-1} on the low-dimensional metals $TaSe_3$ and $NbSe_3$. The A_g spectra exhibit numerous closely spaced lines corresponding to vibrational modes with displacement vectors perpendicular to the chain axis. To interpret these spectra we have made direct use of the bond-strength results of our lattice dynamical model for $ZrSe_3$, which has a similar prismatic chain structure. The broad correlations obtained between the data and the calculated frequencies indicate that the C_{2v} symmetry of the chain is preserved in the B_g vibrations; that strong metal-selenium bonds exist which link the chains into layers; and that Se-Se pairing within the chains is weaker and more varied in $TaSe_3$ and $NbSe_3$ than in $ZrSe_3$.

INTRODUCTION

In our previous papers we have described a valence force lattice dynamical model for several structurally related MX_3 compounds (M = Ti,Zr,Hf; X = S,Se,Te),[1-3] which indicated the presence of one- as well as two-dimensional features in the phonon spectrum. $TaSe_3$ and $NbSe_3$ have a similar prismatic chain structure, although the number of chains passing through the primitive cell is two or three times as large as that in $ZrSe_3$ and the side linkages between the chains are more complex. The large number of atoms in the primitive cell (16 for $TaSe_3$ and 24 for $NbSe_3$) yields a rich Raman spectrum composed of numerous closely spaced lines; the metal-selenium and Se-Se bonds between the chains complicate the interpretation of these spectra. We have found that the key to interpreting the Raman data on $TaSe_3$ and $NbSe_3$ is the lattice dynamical model for the simpler $ZrSe_3$ structure, which gives a starting point for estimating bond strengths and evaluating bonding trends. Two principal results have been obtained by applying this model: $TaSe_3$ and $NbSe_3$ have been shown to be composed of inequivalent prismatic chains distinguished by the degree of Se-Se pairing within the chain, and the phonon system is mixed-dimensional, that is, it preserves features of the isolated chain as well as the layered crystal structure. The existence of Se-Se bonding between the chains has not as yet been established, but a detailed dynamical model for the low-frequency vibrational modes might resolve this question.

In $TaSe_3$ and $NbSe_3$, wedged-shaped prisms are stacked base to base to form chains along the z-axis.* The metal atom at the center of each prism is coordinated to six selenium atoms at the corners and to two other selenium atoms in neighboring chains. These metal-selenium linkages between chains define a set of weakly interacting layers that are parallel to (110) in $TaSe_3$ and to (010) in $NbSe_3$.[4,5] The combination of chains and layers within the crystal suggests the use of the correlation method to relate the internal vibrations of the chain to those of the layer or crystal. Since the chain, layer, and crystal symmetries (C_{2v}, C_{2h}, and C_{2h}, respectively) of $TaSe_3$ and $NbSe_3$ are identical to those of $ZrSe_3$, we can use the correlation diagram previously worked out for $ZrSe_3$.[1] The vibrational decompositions of the total representations of the chain and the crystal are therefore given by

$$\Gamma_{chain} = \underset{xz}{A_2} + \underset{z;yz}{3B_1} + \underset{y;x^2,y^2,z^2}{4A_1} + \underset{x,R_z;xy}{4B_2}, \tag{1}$$

$$\Gamma_{TaSe_3} = \underset{z}{8A_u} + \underset{xz;yz}{8B_g} + \underset{x,y}{16B_u} + \underset{R_z;x^2,y^2,z^2,xy}{16A_g}, \tag{2}$$

and

$$\Gamma_{NbSe_3} = 12A_u + 12B_g + 24B_u + 24A_g, \tag{3}$$

---

*We have chosen the first crystallographic setting for the monoclinic ($P2_1/m - C_{2h}^2$) $TaSe_3$ and $NbSe_3$ structure.

where we have written the transformation properties below each ireducible representation. It should be noted that the z-axis of the chain coincides with the z-axes of the crystals but that the x- and y-axes of the chain differ from the x- and y-axes of the crystals. The correlation diagram also shows that the B_g modes are polarized along the z-axis, whereas the A_g modes have eigenvectors only in the xy plane.

RAMAN SPECTRA

$TaSe_3$ and $NbSe_3$ grow as long needles or wires up to 5 cm in length and 75 μm in width. Although the length of the needle is parallel to the chain axis of the crystal, the layer surfaces ((110) in $TaSe_3$ and (010) in $NbSe_3$) cannot be readily established by mechanical cleavage. Samples of the two crystals were therefore mounted for light-scattering experiments unoriented in the xy plane. To prevent thermal damage to the small samples from the focused laser radiation, the crystals were joined to an aluminum substrate with a liquid metal alloy. The Raman spectra were obtained with a Spectra Physics 4 W argon-ion laser, an Amici prism filter for isolating the laser line, a Spex double monochromator with holographic gratings and polarization scrambler, and photon counting electronics. Because of the irregular scattering surface of the crystals, a large angle of incidence ($\approx 75^o$) was used to minimize the background level of the scattered light. Two scattering geometries, illustrated in Figure 1, were chosen to distinguish the A_g from the B_g vibrations; but note that the B_g spectrum in Figure 1 also contains many A_g features, since the electric vector of the incident laser beam has a component lying in the xy plane of the crystal.

The A_g spectrum of $ZrSe_3$ consists of five or six lines, three of which are relatively strong and appear at high frequencies (177 - 302 cm^{-1}).[1,6] If the interchain coupling in $TaSe_3$ and $NbSe_3$ were weak, their A_g spectra would be similar to that of $ZrSe_3$. However, the complex A_g spectra of $TaSe_3$ and $NbSe_3$ in Figures 1 and 2 demonstrate that the $4A_1 + 4B_2$ internal vibrations of the chain are substantially altered by interchain bonding. The B_g spectrum of $ZrSe_3$, on the other hand, has only a single line at 77 cm^{-1}, identified as one of the shearing vibrations of the chain.[2] The frequency of this vibration is controlled by the strength of the principal metal-selenium bond within the chain. This line is also expected to appear in the $TaSe_3$ and $NbSe_3$ spectra, since the chain symmetry probably continues to dominate in the B_g vibrations. Figure 1 shows one clear feature at 129 cm^{-1}. If

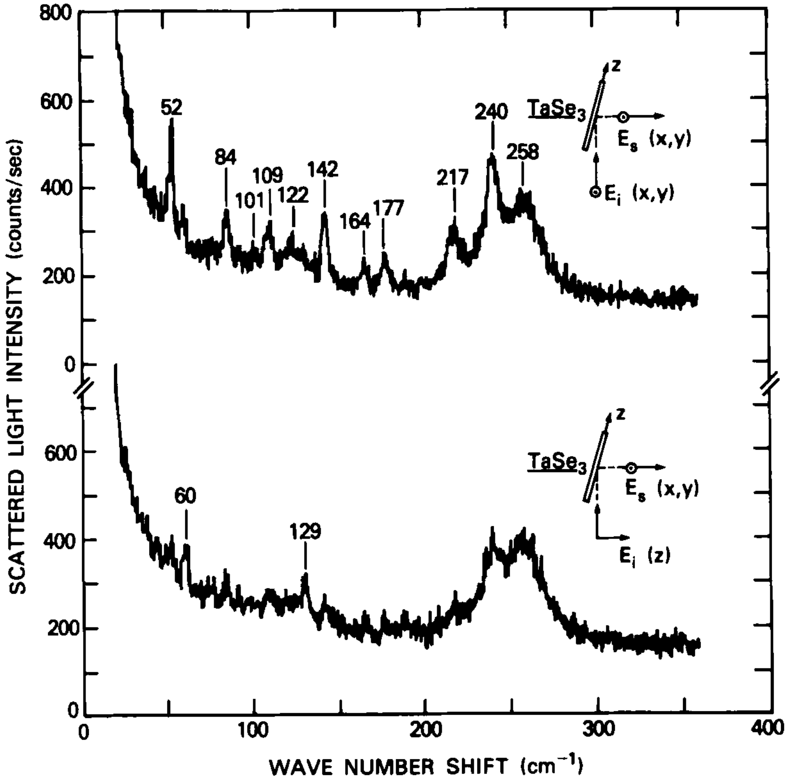

FIGURE 1 Raman spectrum of $TaSe_3$ at room temperature (5145 A laser line)

this feature is the shearing vibration of the chain, then the metal-selenium intrachain bond is stronger in $TaSe_3$ than in $ZrSe_3$. This tentative conclusion will be supported by our lattice dynamical model, which we now proceed to discuss.

BONDING AND LATTICE DYNAMICS

Although the starting point for interpreting the spectra of Figures 1 and 2 is the $ZrSe_3$ force model, a few comparisons of bond length in the three structures will prove to be useful. First, the Se-Se bond length within the chain is longer and more variable in $TaSe_3$ (2.58 A, chain I; 2.90 A, chain II) and $NbSe_3$ (2.50 A, chain I; 2.92 A, chain II; 2.37 A, chain III) than in $ZrSe_3$ (2.35 A). Second, the nearest-neighbor

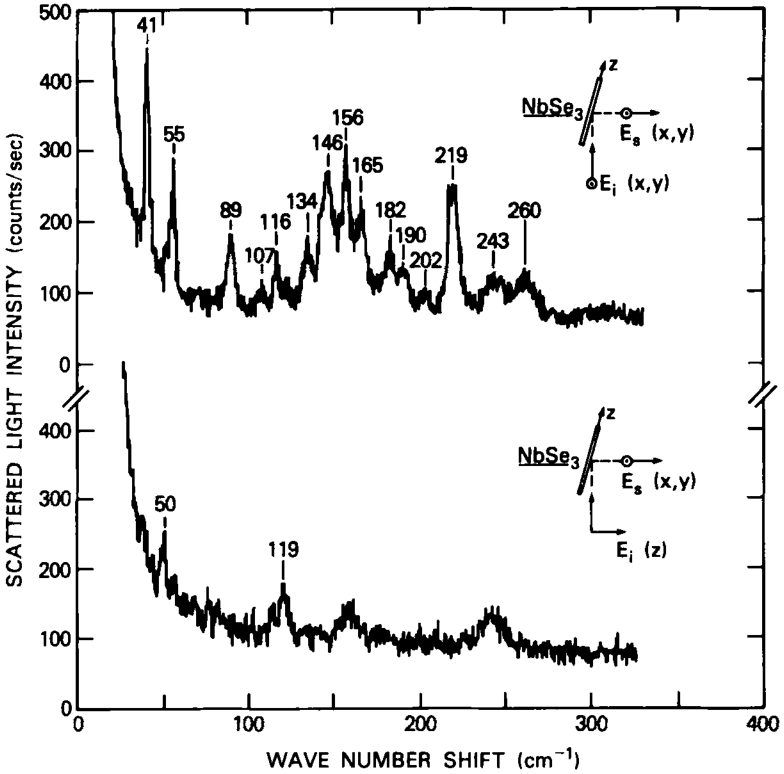

FIGURE 2 Raman spectrum of $NbSe_3$ at room temperature (5145 A laser line)

metal-selenium bonds within and between the chains are approximately 0.1 A shorter on average in $TaSe_3$ and $NbSe_3$ than they are in $ZrSe_3$. Finally, the Se-Se bonds between the chains and within a layer are much shorter in $TaSe_3$ (2.65 A) than they are in $ZrSe_3$ (3.04 A). These changes in bond length have been found to correlate well with changes in the force constants when the $ZrSe_3$ model is applied to $TaSe_3$.

For simplicity, we have eliminated the bond-angle restoring forces in the $ZrSe_3$ model, which affect only the very low frequency vibrations. The central force model that remains consists of a metal-selenium force constant within the chain, C_w; a Se-Se force constant within the chain, C_w'; a metal-selenium force constant between chains, C_b; and a van der Waals force constant, C_v, linking all pairs of Se atoms between chains. To this basic model for TaSe$_3$ has been added a second force constant within the chain, C_w'', to distinguish the strength of Se-Se pairing in chain II from that in chain I. A Se-Se interchain force constant, C_b', has also been added to take into account the special arrangement of the chains in TaSe$_3$.

The first calculation of the A_g frequencies of TaSe$_3$ was carried out with the force constants for ZrSe$_3$ and with $C_w'' = C_w'$ and $C_b' = 0$. The calculation yielded an A_g doublet at 308/300 cm^{-1} and opened up a gap in the A_g spectrum down to 144 cm^{-1} (compare Figure 1). Reducing C_w' from 2.0 x 10^5 dyn/cm to 1.3 x 10^5 dyn/cm brought the doublet down to 255/245 cm^{-1} but did not affect the A_g mode at 144 cm^{-1}. The gap in the calculated spectrum could only be closed by increasing C_w and C_b in roughly equal proportions; the agreement between the model and the two highest A_g frequencies (240 and 258 cm^{-1}) was further improved by reducing C_w''. Table 1 summarizes the best fit obtained with the following force constants: $C_w = C_b = 9.8 \times 10^4$, $C_w' = 1.1 \times 10^5$, $C_v = 7.2 \times 10^2$, $C_b' = 0$, and $C_w'' = 4 \times 10^4$ dyn/cm. Increasing C_b' from zero to 5 x 10^4 dyn/cm raised several of the low frequency A_g modes but did not appreciably affect the best-fit values of C_w, C_w', C_b, and C_w''. A more detailed force model, one that includes bond-angle restoring forces, will be required to determine whether C_b' is important to the lattice dynamics of TaSe$_3$. The agreement in Table 1 between the calculated frequencies and the Raman data is seen to deteriorate at the lower frequencies. This is an expected result since the low frequency modes in the ZrSe$_3$ structure were found to be sensitive to bond-angle restoring forces. We conclude from the TaSe$_3$ model that the strength of the intrachain Se-Se bond is different in the two chains, that the metal-selenium bond is stronger in TaSe$_3$ than in ZrSe$_3$, and that the B_g modes are almost independent of the coupling between the chains. A comparison between the displacement vectors of the B_g modes in TaSe$_3$ and those of an isolated chain shows that they are nearly identical. The layering of the TaSe$_3$ structure is established by the strength of the interchain Ta-Se bond ($C_b = C_w \approx C_w'$), which joins the chains into layers along (110).

The NbSe$_3$ spectrum of Figure 2 displays many of the features of the TaSe$_3$ spectrum of Figure 1. While we have not calculated the A_g frequencies for NbSe$_3$, based on the modified ZrSe$_3$ model, two tentative conclusions can be reached. The triplet at 219/243/260 cm^{-1} in Figure 2 is probably the remnant of the diatomic mode in ZrSe$_3$ and corresponds to the 240/258 cm^{-1} doublet in TaSe$_3$. (Since there are three different chains in the unit cell of NbSe$_3$, the diatomic mode will become a triplet in NbSe$_3$.) In addition, the line at

Table 1 Raman data (295 K) for $ZrSe_3$ and $TaSe_3$ compared with the calculated frequencies (cm^{-1}) of the valence force[a] or central force models

Vibrational symmetry		$ZrSe_3$		$TaSe_3$	
Chain	Crystal	Raman	Calc.[a]	Raman	Calc.
A_1(diatomic)	A_g	302	303	258 240	257 240
B_1(rigid-sublattice)	B_g	-	177	- -	208 207
A_1	A_g	236	240	- 217	230 218
B_2	A_g	-	176	- 177	191 187
A_1	A_g	177	140	164 142	169 153
B_2	A_g	106.5[b]	96	122 109	135 128
A_2	B_g	77	86	129 -	138 137
B_1	B_g	-	85	- -	137 136
A_1(acous./rigid-chain)	A_g	78	71	101 84	77 73
B_2(rot./libration)	A_g	50	50	60 52	24 23
B_2(acous./rigid-chain)	A_g	-	16	- -	18 11
B_1(acous./rigid-chain)	B_g	-	20	- -	17 11

[a] Reference 2
[b] Reference 6

119 cm^{-1} in the B_g spectrum of Figure 2 is probably the shearing mode of the chain; its relatively high frequency suggests that the metal-selenium bond within the chain is stronger than that in $ZrSe_3$. The lattice dynamics of $NbSe_3$ should generally be similar to the results obtained for $TaSe_3$.

REFERENCES

1. T.J. Wieting, A. Grisel, F. Levy, and Ph. Schmid, in: Quasi-One-Dimensional Conductors I, Lecture Notes in Physics, Vol. 95 (Springer-Verlag, Berlin, 1979), p. 354.
2. A. Grisel, F. Levy, and T.J. Wieting, Physica, 99B, 365 (1980).
3. T.J. Wieting, A. Grisel, and F. Levy, Physica, 105B, 366 (1981).
4. F. Hulliger, Structural Chemistry of Layer-Type Phases, edited by F. Levy (D. Reidel, Dordrecht, 1976), p. 251.
5. J.L. Hodeau, M. Marezio, C. Roucau, R. Ayroles, A. Meerschaut, J. Rouxel, and P. Monceau, J. Phys. C, 11, 4117 (1978).
6. A. Zwick and M.A. Renucci, Phys. Status Solidi B, 96, 757 (1979).